Loss of miRNA biogenesis induces p19^{Arf}-p53 signaling and senescence in primary cells

Rajini Mudhasani,[1] Zhiqing Zhu,[1] Gyorgy Hutvagner,[2] Christine M. Eischen,[4] Stephen Lyle,[3] Lisa L. Hall,[1] Jeanne B. Lawrence,[1] Anthony N. Imbalzano,[1] and Stephen N. Jones[1,3]

[1]Departments of Cell Biology, [2]Biochemistry and Molecular Pharmacology, and [3]Cancer Biology, University of Massachusetts Medical School, North Worcester, MA 01655
[4]Department of Pathology, Vanderbilt University School of Medicine, South Nashville, TN 37232

Dicer, an enzyme involved in microRNA (miRNA) maturation, is required for proper cell differentiation and embryogenesis in mammals. Recent evidence indicates that Dicer and miRNA may also regulate tumorigenesis. To better characterize the role of miRNA in primary cell growth, we generated Dicer-conditional mice. Ablation of Dicer and loss of mature miRNAs in embryonic fibroblasts up-regulated p19^{Arf} and p53 levels, inhibited cell proliferation, and induced a premature senescence phenotype that was also observed in vivo after Dicer ablation in the developing limb and in adult skin. Furthermore, deletion of the Ink4a/Arf or p53 locus could rescue fibroblasts from premature senescence induced by Dicer ablation. Although levels of Ras and Myc oncoproteins appeared unaltered, loss of Dicer resulted in increased DNA damage and p53 activity in these cells. These results reveal that loss of miRNA biogenesis activates a DNA damage checkpoint, up-regulates p19^{Arf}-p53 signaling, and induces senescence in primary cells.

Introduction

microRNAs (miRNAs) are single-stranded RNA molecules that regulate the expression of messenger RNA. miRNAs are generated from RNA transcripts that are exported into the cytoplasm, where the pre-miRNA molecules undergo final cleavage by Dicer, a ribonuclease III–like enzyme. The mature miRNAs assemble into ribonucleoprotein silencing complexes (RISCs) and guide the silencing complex to specific mRNA molecules (Du and Zamore, 2005).

In mammals, Dicer plays important roles in cell differentiation and tissue morphogenesis (Harfe et al., 2005; Muljo et al., 2005; Yang et al., 2005; Andl et al., 2006; Harris et al., 2006), and ablation of Dicer in mice induces embryonic lethality at E6–E7 (Bernstein et al., 2003). Previous studies indicate that Dicer loss correlates with reduced cell proliferation in mouse embryonic stem (ES) cells (Kanellopoulou et al., 2005; Murchison et al., 2005) or increased apoptosis in specific tissues during development (Muljo et al., 2005; Andl et al., 2006; Harris et al., 2006), yet global repression of miRNA maturation in cultured cells has also been shown to promote cellular growth, transformation, and tumorigenesis (Kumar et al., 2007). Recently, the miR-34 family of miRNAs was found to be a direct transcriptional target of the p53 tumor suppressor (Bommer et al., 2007; He et al., 2007; Raver-Shapira, et al., 2007), indicating a potential role for miRNAs in tumor suppression.

To better understand the role of miRNAs in regulating cell growth, we generated mice bearing conditional alleles of *Dicer* and examined the effects of loss of miRNA biogenesis on primary cell growth. Dicer ablation caused a rapid onset of cell senescence in mouse embryonic fibroblasts (MEFs) in vitro and in developing and adult mouse tissues in vivo. Furthermore, inhibition of miRNA maturation in primary cells induced H2A.X staining, up-regulation of p19^{Arf} and p53 tumor suppressor protein levels, phosphorylation of p53, and induction of p53 target genes involved in regulating cell growth and senescence. Deletion of either Ink4a/Arf or p53 genes rescued the cells from premature senescence induced by Dicer ablation. These results reveal that loss of miRNA biogenesis in primary cells induces DNA damage and a premature cell senescence that is mediated by the p19^{Arf}-p53 signaling axis.

Results and discussion

We performed gene targeting in ES cells using a *Dicer* gene replacement vector, and two Dicer alleles were recovered after

R. Mudhasani and Z. Zhu contributed equally to this paper.

Correspondence to Stephen N. Jones: stephen.jones@umassmed.edu

Abbreviations used in this paper: Ad, adenovirus; dpi, days post induction; ES, embryonic stem; FACS, fluorescence-activated cell sorting; MEF, mouse embryonic fibroblast; miRNA, microRNA; SA-βgal, senescence-associated β-galactosidase; SAHF, senescence-associated heterochromatin foci; wt, wild type.

The online version of this paper contains supplemental material.

The Rockefeller University Press $30.00
J. Cell Biol. Vol. 181 No. 7 1055–1063
www.jcb.org/cgi/doi/10.1083/jcb.200802105

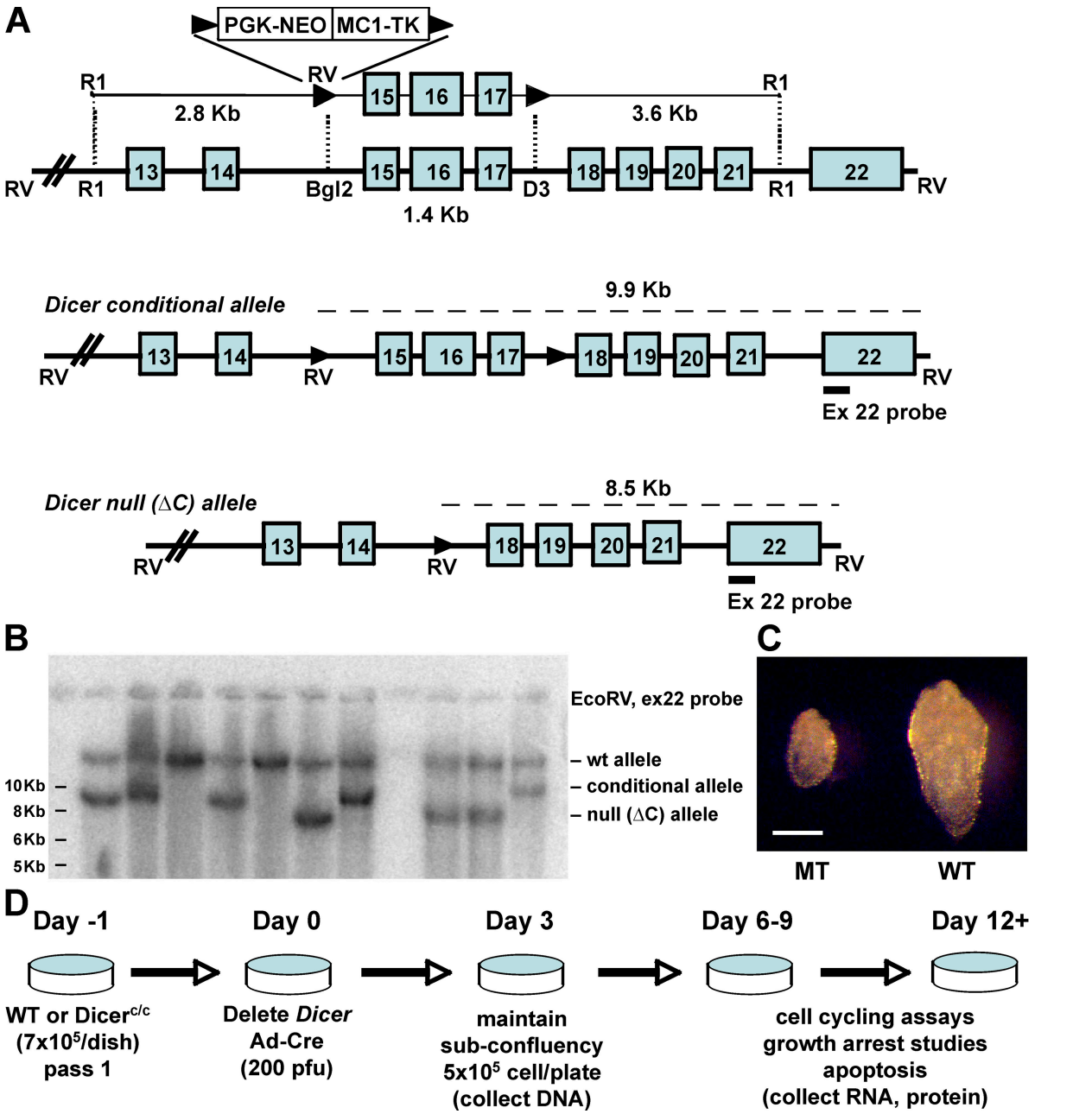

Figure 1. **Generation of Dicer$^{c/c}$ mice and embryonic fibroblasts.** (A) Dicer exons 15–17 flanked with loxP sites in targeted ES cells. Cre-excision generates a conditional allele (middle) and a null allele deleted for Dicer exons 15–17 (bottom). (B) Southern analysis of F1 mice indicates transmission of both Dicer-modified alleles. Marker band positions are shown at left. (C) Phenotype of Dicer wild-type (WT) and mutant (MT) mice at E7 (darkfield image). Bar, 250 μM. (D) Strategy for creating and analyzing Dicer-ablated MEFs.

Cre excision of the drug selection markers (Fig. 1 A). ES clones bearing either a Dicer allele with exons 15–17 flanked by loxP sites, or a Dicer allele deleted for exons 15–17 were isolated. Excision of these exons should result in a Dicer-null allele, as these sequences encode the PAZ domain required for Dicer recognition of pre-miRNA molecules. Furthermore, Cre deletion places the remainder of coding sequences, including those encoding the RNase III domains, in an incorrect translational frame. Blastocyst injections were performed and germline transmission of either the Dicer-null (ΔC) allele or the Dicer-conditional (C) allele was achieved (Fig. 1 B).

To confirm that deletion of the floxed exons results in loss of Dicer function, we intercrossed Dicer$^{+/\Delta C}$ mice. Genotyping of embryos harvested from the Dicer$^{+/\Delta C}$ crosses at varying times during gestation indicated lethality of Dicer$^{\Delta C/\Delta C}$ mice before E8.5 (Fig. S1 A, available at http://www.jcb.org/cgi/content/full/jcb.200802105/DC1), and recovery of E7 embryos revealed that 25% (5/20) of the embryos were smaller than wild-type (wt) E7 embryos (Fig. 1 C). This phenotype is similar to that reported for a loss of function Dicer allele in mice (Bernstein et al., 2003), confirming that deletion of the floxed region generates a Dicer-null allele.

Mice heterozygous for the Dicer-conditional allele (Dicer$^{+/c}$) were crossed to produce Dicer$^{c/c}$ mice. The expected Mendelian ratio for each genotype was recovered, and Dicer$^{c/c}$ mice were indistinguishable from wt mice. In addition, multiple lines of Dicer$^{c/c}$ or Dicer$^{+/c}$ MEFs were generated from these matings.

To ablate Dicer function, Cre recombinase was transiently expressed in Dicer$^{c/c}$ MEFs by infecting cells with recombinant adenovirus (Ad) encoding Cre. Infection with 200 plaque-forming units of Ad-Cre failed to alter the growth of wt MEFs, yet resulted in a greater than 95% transduction of Cre activity as judged by excision of flox-stop reporter gene alleles in control Gt(ROSA)26 MEFs (unpublished data). Dicer$^{c/c}$ MEFs or control wt and Dicer$^{c/+}$ MEFs were plated 24 h before Ad-Cre or Ad-control (Ad-βgal reporter virus) infections, and cells maintained at subconfluent densities through 12 or longer days post-induction (dpi) (Fig. 1 D). Southern analysis demonstrated Cre deletion of the floxed exons at 3 dpi (Fig. S1 B). RT-PCR performed on RNA isolated from Dicer$^{c/c}$ cells revealed loss of exons 15–17 and reduced amounts of Dicer mRNA, suggesting that deletion of exons 15–17 also reduced message stability (Fig. S1 C). To confirm loss of miRNA maturation, we examined the global level of mature miRNAs in Dicer-ablated MEFs. miRNA microarray data revealed that ∼80% of the total mature miRNA molecules were dramatically reduced by 3 dpi, and almost all of the mature miRNA were depleted by day 5 (unpublished data). Quantitative PCR (qPCR) and Northern analysis revealed that the level of select mature miRNAs in Dicer$^{c/c}$ MEFs transduced with exogenous Cre was greatly reduced at 3 dpi (Fig. S1, D and E). Collectively, these results indicate that the addition of Cre to Dicer$^{c/c}$ MEFs efficiently depletes Dicer activity and mature miRNAs.

Dicer$^{c/c}$ MEFs were infected with Ad-Cre or Ad-control (Ad-βgal) and recovered at 9 dpi. As a control, wt MEFs were also infected with Ad-Cre or Ad-control. Fluorescence-activated cell sorting (FACS) analysis of asynchronously growing MEFs revealed that Dicer-ablated MEFs were undergoing less DNA replication than Dicer$^{c/c}$ MEFs infected with control virus, whereas no difference was seen in the growth rate of wt MEFs transduced with Ad-Cre or with Ad-control (Fig. 2 A). Furthermore, Dicer loss results in a reduction in S phase cells without inducing apoptosis (Fig. S2 A, available at http://www.jcb.org/cgi/content/full/jcb.200802105/DC1).

To confirm the reduced growth of MEFs after Dicer ablation, a proliferation assay was performed. MEFs lacking Dicer proliferate far slower than control-infected MEFs or MEFs retaining Dicer (Fig. 2 B). Similar results were obtained in Dicer$^{c/c}$ MEFs after tamoxifen-induced Dicer ablation in Dicer$^{c/c}$ MEFs bearing the CAG-CreER transgene (Hayashi and McMahon, 2002). Furthermore, induction of Cre activity in Dicer$^{c/wt}$ MEFs had no effect on the proliferation of these cells, demonstrating that haploinsufficiency for Dicer does not alter cell growth (Fig. 2 C).

Although Dicer-ablated MEFs grow more slowly than wt MEFs, the Dicer-ablated cells could be passaged several times before the cells stopped dividing and assumed a large, flattened morphology. To determine if these cells were becoming senescent, Dicer$^{c/c}$ MEFs were either mock infected (no virus) or Ad-Cre infected, passaged once at a lower density on 3 dpi, and the media changed every third day. Mock-infected Dicer$^{c/c}$ MEFs displayed normal growth characteristics, whereas Dicer-ablated cells displayed flat cell morphology after 9 d in culture. Harvesting and replating cells in fresh media at higher or lower densities failed to stimulate their growth, and approximately half of the Dicer-null cells failed to attach when replated. Increasing the serum content from 10% to 20% also had no effect on Dicer-null MEFs. After 3 wk in culture, foci of cells would appear and begin to expand on the plates. However, genotyping of foci cells revealed that these were MEFs that had escaped Cre-mediated deletion of the Dicer-conditional allele (unpublished data).

To confirm that Dicer-ablated MEFs were undergoing senescence, the cells were fixed and stained for senescence-associated β-galactosidase (SA-βgal) activity (Campisi, 2003). Little or no staining was detected in the control Dicer$^{c/c}$ plates at 9 dpi, whereas SA-βgal activity was readily apparent in the Dicer-ablated cells (Fig. 2 D). Repeat experiments using triplicate lines of MEFs were performed, and the percentage of cells showing SA-βgal activity was counted in mock-infected or Ad-Cre infected Dicer$^{c/c}$ MEFs (Fig. 2 E). Over 40% of the Dicer-ablated MEFs underwent senescence by day 9, compared with less that 5% senescence in nondeleted MEFs, and Dicer-ablated MEFs displayed a 10-fold increase in senescent cells by day 12. Control experiments revealed no difference in SA-βgal activity in wt MEFs at early or late times post-infection using either Ad-Cre or with Ad-control virus (Fig. S2 B).

Senescent human cells are characterized by the formation of senescence-associated heterochromatin foci (SAHF) (Dimri et al., 1995; Narita et al., 2003). In SAHF, chromatin is dramatically reorganized in an Rb- and p53-dependent manner, resulting in striking DAPI-dense accumulations of heterochromatin (Ye et al., 2007). As expected, the nuclei of Dicer$^{c/c}$ MEFs show DAPI-dense chromatin associated with mouse chromocenters (clustered centromeres from multiple chromosomes) before or after mock infection (Fig. 2 F, left). In contrast, Cre-mediated deletion of Dicer in Dicer$^{c/c}$ cells resulted in 20–30% of the cells displaying very large aberrant clumps of coalesced heterochromatin (Fig. 2 F, right), which is observed only in 1–5% of mock-infected Dicer$^{c/c}$ cells. Although SAHF has not been fully characterized in mouse cells, these DAP1-dense structures in Dicer-ablated cells are reminiscent of the SAHF observed in senescent human cells.

Senescence can be induced by oncogene activation or by DNA damage (Zhang, 2007), and biogenesis of miRNAs in cell lines has been reported to regulate the expression of oncogenes involved in cell growth control (Johnson et al., 2005). To examine the effects of Dicer ablation on Myc and Ras levels, we performed Westerns using Dicer$^{c/c}$ MEFs infected with either Ad-Cre or Ad-control. However, little difference was observed in the levels of the Myc or Ras (Fig. 3 A). In contrast, an increase was readily detected in p53 levels in the Dicer-ablated cells.

To determine if Dicer loss induced DNA damage, we performed immunofluoresence staining with an antibody to histone H2A.X. Numerous H2A.X-positive foci were seen in Dicer-ablated cells at 12 dpi, but not in control-infected Dicer$^{c/c}$ MEFs (Fig. 3 B). To determine if DNA damage coincides with the onset

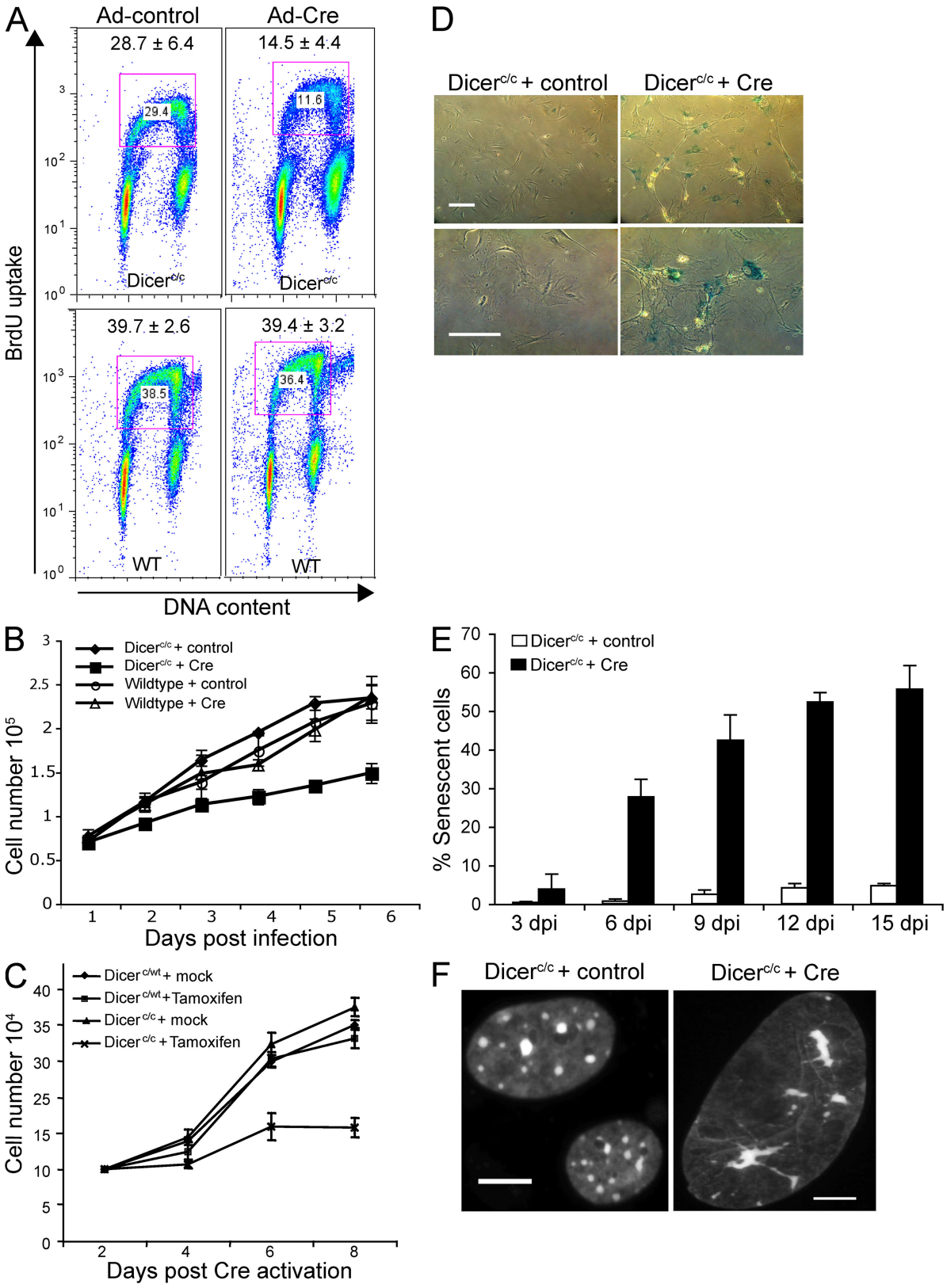

Figure 2. **Reduced primary cell proliferation and premature senescence in Dicer-ablated primary MEFs.** (A) FACS indicates fewer Dicer-ablated cells undergo DNA replication. (B) Proliferation assay of Dicer-wt and Dicer-ablated cells reveals that Dicer loss inhibits cell proliferation. (C) Proliferation assay of Dicer-heterozygous and Dicer-ablated cells after induction of Cre activity. (D) SA-βGal staining of Dicer-wt or Dicer-ablated cells at day 12. Bar, 200 μM. (E) SA-βGal staining of Dicer$^{c/c}$ MEFs after Ad-Cre or Ad-control infection. (F) DAPI-staining of DNA reveals dramatically altered heterochromatin in Dicer-ablated cells (right). Bar, 10 μM.

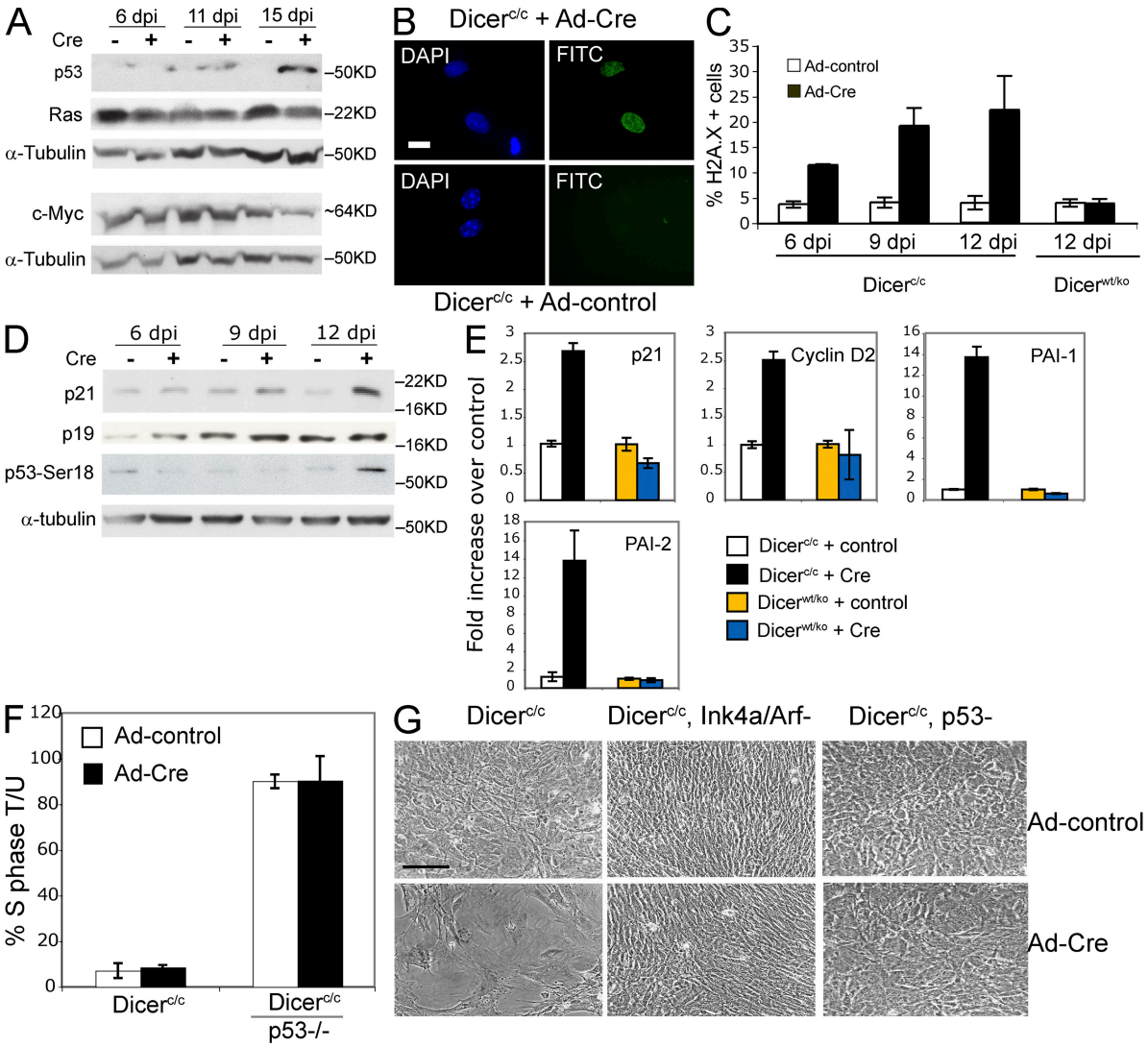

Figure 3. **Dicer ablation induces DNA damage and activates the p19^{Arf}-p53 signaling pathway.** (A) Western analysis of Ras, Myc, and p53 levels in Dicer$^{c/c}$ MEFs either mock infected (−) or Ad-Cre infected (+) at 6, 11, and 15 dpi. Elevated p53 is observed in the Dicer-ablated cells, whereas Myc and Ras levels appear unchanged. Tubulin was used as a loading control for the Ras and p53 blot, as well as for the separate Myc blot. (B) DAPI and H2A.X staining of Dicer-ablated MEFs or control MEFs at 12 dpi. (C) The percentage of H2A.X-positive cells is increased in Dicer-ablated MEFs over time. Bar, 20 μM. (D) Western analysis of p21, p19Arf, and phosphorylated p53-Ser18 levels in Dicer$^{c/c}$ MEFs mock infected (−) or Ad-Cre infected (+) at 6, 9, and 12 dpi. Elevated levels of p21 and p19Arf, and p53 activation in the Dicer-ablated cells. Tubulin is the loading control. (E) qPCR analysis of p53 target gene expression reveals that Dicer loss up-regulates p21, CyclinD2, PAI-01, and PAI-2. (F) Adriamycin induces a p53-mediated arrest in Dicer-ablated cells. (G) Morphology of Dicer$^{c/c}$ MEFs at day 12 after Ad-control or Ad-Cre infection. Dicer$^{c/c}$ MEFs either wt (left panels) or deleted for either In4a/Arf (center panels) or p53 (right panels). Deletion of Ink4a/Arf or p53 inhibited the premature senescence of Dicer-ablated MEFs. Bar, 400 μM.

of senescence, we performed H2A.X staining on Dicer$^{c/c}$ MEFs and Dicer-heterozygous MEFs at various times after Ad-Cre infection. Increased DNA damage could be readily detected at 6 dpi in Dicer$^{c/c}$ MEFs after infection with Ad-Cre. No difference was seen in the levels of DNA damage in control-infected Dicer-heterozygous MEFs, confirming that the DNA damage in Dicer-ablated MEFs was due to loss of Dicer function (Fig. 3 C).

DNA damage–induced senescence is mediated, in part, by the p19^{Arf} and p53 tumor suppressors, and by the cdk inhibitor p21, a downstream mediator of p53 activity. Therefore, we examined the levels of these proteins in Dicer-ablated MEFs (Fig. 3 D). The data reveal an increase in p19^{Arf} levels over time, with higher levels of p19^{Arf} consistently found in cells lacking Dicer. Similarly, p21 protein levels are higher in Dicer-ablated MEFs, suggesting that premature senescence in Dicer-ablated MEFs may be due to induction of p19^{Arf}-p53-p21 signaling. In addition, activation of p53 could also be detected in Dicer-ablated MEFs as judged by p53-serine18 phosphorylation (Webley et al., 2000). Control experiments with wt MEFs confirmed that Ad-Cre transduction alone does not alter p19 or p53ser18 phosphorylation (Fig. S2 C). Furthermore, Dicer loss resulted in increased expression of p53 target genes associated with p53-mediated cell senescence, including *p21*, *PAI-1*, *PAI-2*, and *CylinD2* (Fig. 3 E).

Thus, loss of miRNA biogenesis in primary cells results in increased DNA damage, up-regulation of p19^{Arf}-p53 signaling,

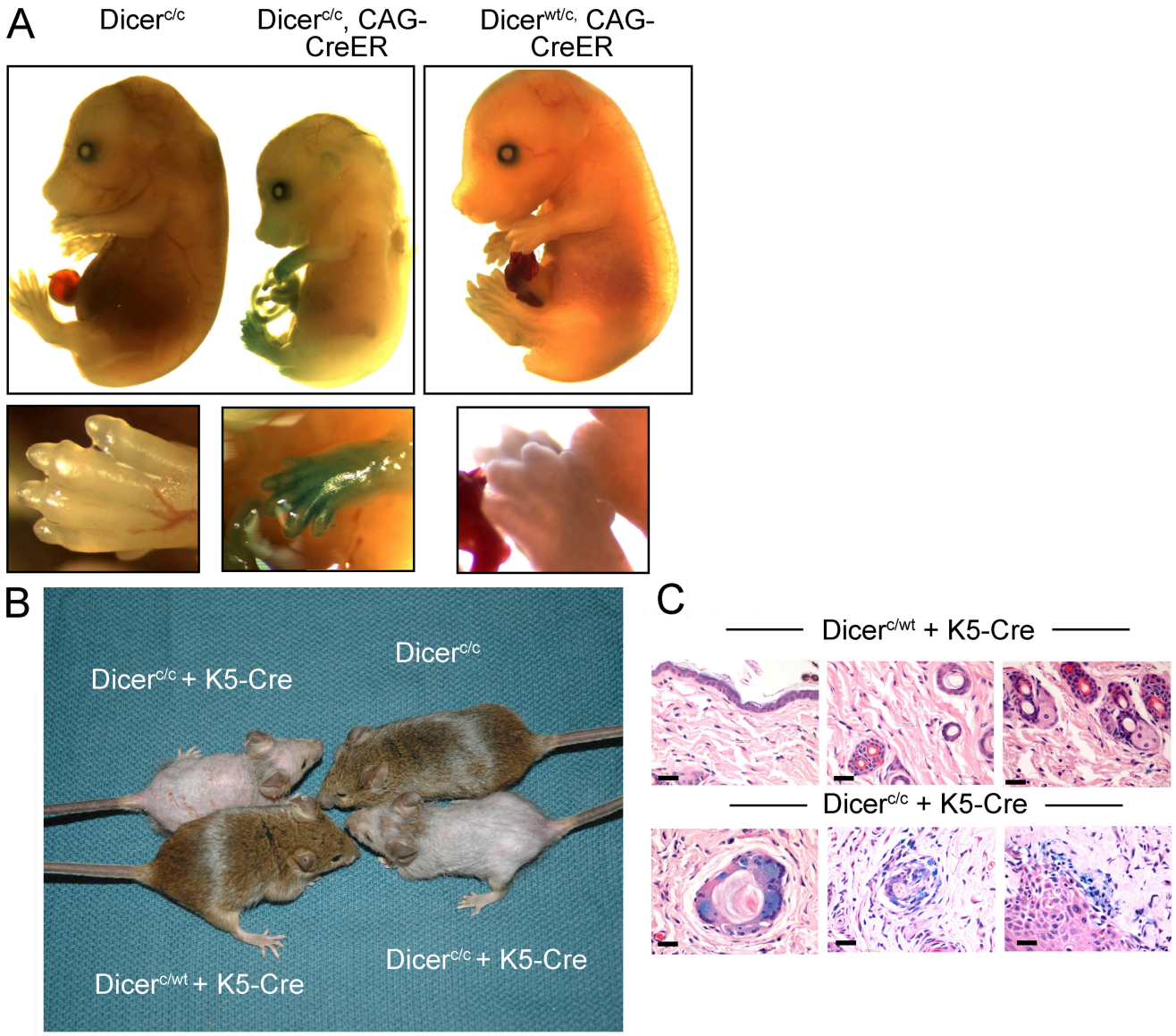

Figure 4. **Deletion of Dicer induces cellular senescence in vivo.** (A) SA-βgal staining of embryos after tamoxifen-induced Dicer ablation in utero reveals that loss of Dicer promotes senescence in E16 developing limbs. No senescence is seen in Dicer$^{c/wt}$ embryos (right). (B) 3-mo-old sibling mice derived from K5-Cre x Dicer$^{c/c}$ crosses. Dicer ablation results in fur loss after 12 wk. (C) Skin histopathology of mice retaining or ablated for Dicer by the K5-Cre transgene. Hematoxylin and eosin staining of skin sections followed by staining for SA-βGal activity. Dicer-ablated cells (bottom panels) are larger in size and display SA-βGal activity. Bar, 100 μM.

p53 activation, induction of p53 target genes, and subsequent cell senescence. To confirm that MEFs lacking Dicer could undergo DNA damage–induced growth arrest, we examined the response of Dicer-ablated MEFs to adriamycin. FACS analysis in Dicer-ablated cells revealed a large reduction in S phase after DNA damage (Fig. 3 F). As expected, DNA replication in p53-null MEFs was only slightly reduced by adriamycin. In contrast, there was no difference in the growth arrest of MEFs lacking Dicer.

To confirm Dicer loss induces premature senescence by activation of the p19^{Arf}-p53 pathway, we bred Dicer$^{c/c}$ mice with either Ink4a/Arf-null mice (Serrano et al., 1996) or with p53-null mice (Donehower et al., 1992) and generated Dicer$^{c/c}$, Ink4a/Arf-null MEFs and Dicer$^{c/c}$, p53-null MEFs. As expected, Dicer$^{c/c}$ MEFs lacking either Ink4a/Arf or p53 proliferated faster than Dicer$^{c/c}$ MEFs. Deletion of Dicer by Ad-Cre again induced senescence in a majority of Dicer$^{c/c}$ MEFs by 12 dpi. However, absence of either Ink4a/Arf or p53 in Dicer$^{c/c}$ cells fully rescued the Dicer-ablated MEFs from premature senescence (Fig. 3 G). Dicer-ablated cells lacking either Ink4a/Arf or p53 expanded to fill the plates and could be passaged multiple times in culture. Analysis of senescence marker gene expression was performed using total RNA isolated from wt and Ink4a/Arf-null MEFs that retained or lost Dicer. Increased p16 and p19^{Arf} expression and expression of the senescence-associated, p53-target genes *p21*, *PAI-1*, and *PAI-2* was observed in MEFs at 10 d post ablation (Fig. S2 D). Dicer ablation in Ink4a/Arf-null MEFs did not alter the expression of *p21*, *PAI-1*, or *PAI-2*. As p19^{Arf} and the p53

downstream effectors p21 and PAI-1 are major regulators of senescence in mouse cells (Sharpless et al., 2004; Jackson and Pereira-Smith, 2006; Kortlever et al., 2006), these data provide genetic proof that a global reduction of miRNAs induces a $p19^{Arf}$-p53–dependent premature senescence in primary cells.

Dicer regulates cell proliferation and morphogenesis in several tissues in mice, including the developing limb (Harfe et al., 2005) and hair follicle (Andl et al., 2006). To confirm that Dicer prevents cell senescence in vivo, we crossed $Dicer^{c/c}$ or $Dicer^{wt/wt}$ female mice with CAG-CreER transgenic $Dicer^{c/c}$ males, and induced embryonic Cre activation by intraperitoneal tamoxifen injection (3 mg/40 g bodyweight) in females at day 8.5 and 11.5 of pregnancy. Embryos (n = 26) were isolated at E14–E16, genotyped, and stained for SA-βgal activity. Cre-deletion of Dicer in CAG-CreER transgenic, $Dicer^{c/c}$ embryos was confirmed by PCR (Fig. S3 A, available at http://www.jcb.org/cgi/content/full/jcb.200802105/DC1). The results demonstrate senescence in cells of the developing limbs in 13 of 13 Cre-transgenic $Dicer^{c/c}$ mice (Fig. 4 A). No senescence was detected in the 13 $Dicer^{c/c}$ embryos lacking the Cre transgene, or in Cre-transgenic $Dicer^{c/wt}$ heterozygous mice. In addition, we crossed $Dicer^{c/c}$ mice with K5-Cre transgenic mice that express Cre in keratinocytes and in skin epidermis (Zhou et al., 2002), and examined the follicular cells of K5-Cre+, $Dicer^{c/c}$ mice for signs of senescence. All K5-Cre $Dicer^{c/c}$ mice displayed loss of hair and a roughening of the epidermis after 2–3 mo of age (Fig. 4 B), in keeping with a proposed role for miRNA in the maintenance of hair follicles (Andl et al., 2006). K5-Cre transgene function in skin was confirmed using the *Gt(ROSA)26Sor*^{tm1Sor}/J mouse (Fig. S3 B). Skin was isolated from K5-Cre+, $Dicer^{c/c}$ mice and from K5-Cre+, $Dicer^{+/c}$ control mice, fixed, and stained for histological analysis, and for SA-βgal activity (Fig. 4 C). Analysis of genomic DNA in K5-Cre+, $Dicer^{c/c}$ mice documented ablation of Dicer specifically in skin (Fig. S3 C). Fewer and much larger cells were present in the follicular epidermis of mice ablated for Dicer, and SA-βgal activity could be detected in these cells (Fig. 4 C). Collectively, these data reveal that loss of Dicer can induce a cell senescence phenotype in vivo in embryos and in adult mice, confirming that the premature senescence observed in MEFs after inhibition of miRNA maturation is not an artifact of culture.

Recent reports have prompted interest in the potential role of miRNA in cancer. Overexpression of specific miRNAs has been associated with several types of human cancer (Volinia et al., 2006; Voorhoeve et al., 2006; Brueckner et al., 2007). In contrast, impaired miRNA processing increased the tumorigenic potential of mouse adenocarcinoma cells in orthotopic transplantation experiments, and increased the tumor burden of mice bearing a conditional activated allele of K-Ras (Kumar et al., 2007). These findings indicate that loss of miRNA processing and an overall reduction in miRNA enhances tumorigenesis. Very recently, the Myc oncoprotein was found to inhibit expression of select miRNAs that have anti-tumorigenic properties in lymphoma cells, offering further support for a role for miRNAs in tumor suppression (Chang et al., 2008).

Our data reveal that loss of miRNA biogenesis induces a DNA damage checkpoint in certain primary cells, which promotes $p19^{Arf}$-p53–dependent cellular senescence. As p53-mediated senescence has been reported to be an important facet of p53 tumor suppression (Braig et al., 2005; Chen et al., 2005), loss of p53 signaling should greatly facilitate the tumorigenic potential of cells with reduced presence of mature miRNAs. Further experiments exploring the effects of p19 or p53 loss on the role of Dicer and miRNA processing in normal cell growth and in tumorigenesis are presently ongoing.

Materials and methods

Generation of Dicer-conditional mice and Dicer-null mice

A gene replacement vector was constructed by conventional cloning means using 129SV/J genomic DNA fragments that contained exons 15–17 of Dicer, with 2.8 Kbp of 5′ flanking DNA sequence and 3.6 Kbp of 3′ flanking DNA sequence. LoxP sites were inserted to flank Dicer exons 15–17, and a positive/negative drug selection cassette was inserted adjacent to exon 15 in a Bgl2 site. After electroporation of the linearized targeting vector into AB2.2 ES cells (129S7 strain) and G418 drug selection, multiple targeted ES cells were expanded, and a Cre-expression plasmid was transiently introduced into the ES cells to delete the drug selection cassettes. Selection of the cells in FIAU resulted in the recovery of individual ES clones that either retained the floxed exons 15–17 or deleted these exons in the targeted allele, as demonstrated by Southern analysis and by PCR. Several ES cell clones that underwent deletion of the floxed exons or that retained floxed exons 15–17 were used to generate chimeric mice by microinjection of the ES cells into C57BL/6 mouse blastocysts. Germline transmission of Dicer-null (ΔC) allele and the Dicer-conditional (c) allele was achieved by breeding high degree chimeric mice to C57BL/6 mice. Genotyping of genomic DNA isolated from tail biopsies of the agouti offspring was performed by Southern analysis performed using an EcoRV digest and a Dicer exon 22 probe to confirm inheritance of the Dicer modified alleles. $Dicer^{c/c}$ mice bearing the CAG Cre-ER transgene ($Dicer^{c/c}$, Cre-ER) or the Keratinocyte5-CrePrm transgene ($Dicer^{c/c}$, K5-Cre) were obtained by crossing $Dicer^{c/c}$ mice with the Cre mice, and by breeding of the resulting $Dicer^{+/c}$, Cre transgene mice with $Dicer^{c/c}$ mice. PCR-based genotyping of Dicer alleles used a combination of three primers: primer 1F-CCAAGATGCAGTGATCATTCC, primer 2F-CCATTGGTGCCAAGACAATG, and primer3R-CAGGCTCCACTCCCTAAC.

Generation of Dicer-conditional embryonic fibroblasts

MEFs were generated from E13.5 embryos recovered from timed matings of $Dicer^{c/c}$ mice and $Dicer^{+/c}$ mice. All studies were conducted using very low passage embryonic fibroblasts (pass 1 – pass 2), maintained in a 37°C, 5% CO_2 incubator in DME supplemented with 10% fetal bovine serum, penicillin, and streptomycin (MEF media). To determine the rates of cell proliferation, multiple lines of wt or $Dicer^{c/c}$ MEFs were seeded at a density of 10^4 cells/cm^2 and plated either in 10-cm plates or 6-well plates. Dicer was deleted from the $Dicer^{c/c}$ cells by infection with 200 pfu of recombinant Ad5-Cre adenovirus. The cells were maintained at subconfluency by passaging as needed, and triplicate plates of each line were harvested for cell cycling studies, for DNA damage studies, and for senescence analysis. Control-infected (Ad-βGal, 200 pfu) or mock-infected (no virus) $Dicer^{c/c}$ MEFs were used as controls for these experiments, as indicated. Ad-Cre virus and Ad-βGal virus were obtained from the Gene Transfer Vector Core at the University of Iowa (Iowa City, IA). Cre recombinase activity was induced in CAG-CreER MEFs by treating the cells with 0.5 μM tamoxifen for 48 h.

Cell growth assays and DNA damage response

Asynchronously growing $Dicer^{c/c}$ MEFs were infected with either Ad-βGal or Ad-Cre virus and plated at equal density (7.5 x 10^5 cells/10-cm dish) on day 5 after infection. 24 h later, 60 μM BrdU was added to the media for 3 h, and the cells were harvested by trypsinization into phosphate-buffered saline (PBS), fixed in 70% ethanol overnight at 4°C, and subsequently stained with BrdU antibody followed by propidium iodide staining. Flow cytometric analysis of DNA synthesis and total DNA content was performed by the UMMS FACS Core and Flowjo software. To determine the rates of cell proliferation, multiple lines of Dicer-wt and Dicer-ablated MEFs were plated in triplicate 3 d after infection at a density of 10^4 cells/cm^2 and counted every 24 h using a Z1 Coulter Particle Counter (Beckman Coulter). Similar results were obtained using Ad-Cre, and pBABE-Cre infection

of Dicer$^{c/c}$ MEFs, and when using tamoxifen activation of Cre in Dicer$^{c/c}$, Cre-ER MEFs. To assess the response of Dicer-ablated cells to DNA damage, three independent lines of Dicer$^{c/c}$ MEFs or Dicer$^{c/c}$, Cre-ER MEFs were recovered on day 3 after Cre-induction, and seeded onto 10-cm plates at a density of 7.5×10^5 cells/10-cm plate. The cells were left untreated or exposed either to 250 µg adriamycin (doxorubicin) for 8 or 16 h. The cells were pulse-labeled with 60 µM BrdU for three more hours and harvested for FACS analysis as described above. Data are presented as a ratio of percentage of cells in S phase for treated versus untreated cells.

Protein analysis

Total protein was isolated from MEF samples in the presence of Urea lysis buffer (8M Urea, 0.1M NaH_2PO_4, 10 mM Tris-HCL, pH 8.0). 60 µg of total protein was electrophoresed through a 10% acrylamide gel followed by transfer onto a PVDF (Immobilon) membrane. Membranes were blocked in TBST containing 2% nonfat dry milk (Bio-Rad Laboratories) before incubation with antibodies. Antibodies were incubated with membranes in the presence of TBST containing 5% nonfat dry milk at 4°C overnight or 1 h at room temperature (tubulin antibody). Excess primary antibody was removed with three 10-min washes of PBST. Secondary antibodies were incubated with membranes for 1 h at room temperature followed by six 10-min washes with TBST to remove excess antibody. Proteins were visualized on the membrane by exposure to Western Lightning chemiluminescent reagent. The following antibodies were used in this study: p53 (Ab-1 and Ab-3; 1:500 each; Calbiochem), p53ser18 (1:1,000 dilution; Cell Signaling Technology), p21 (Santa Cruz Biotechnology, Inc.), p19Arf (1:1,000; Abcam) and α-tubulin (clone B-5-1-2; 1:4,000; Sigma-Aldrich).

RNA isolation and analysis

Total RNA was isolated from MEFs using Trizol reagent (Invitrogen) according to the manufacturer's protocol. 1 µg of RNA was reverse transcribed using Oligo-dT primers and the SuperScript first Strand Synthesis kit (Invitrogen) according the manufacturer's protocol. Gene expression was assessed by PCR (30 cycles, GAPDH, Dicer) and quantitative real-time PCR (p21, p19, PAI-1,PAI-2 p16, 36B4, and GAPDH). Quantitative PCR was performed using SYBR green 2x master mix (QuantiTect SYBR green RT-PCR mix; QIAGEN) and a 3-step cycling protocol (anneal 55–60°C, elongate at 72°C, denature at 94°C). Specificity of primers was verified by dissociation temperature of amplicons. Quantitative PCR results are representative of two or more independent experiments. Primers used for PCR reactions are as follows: PAI-1(F)GCTGCACCCTTTGAGAAAGA, PAI-1(R)-GCCAGGGTTGCACTAAACAT, p19Arf(F)CCCACTCCAAGAGAGGGTTT, p19ARF(R) TCTGCACCGTAGTTGAGCAG, p16(F)ATCTGGAGCAGCATGGAGTC, p16(R)TCGAATCTGCACCGTAGTTG, PAI-2(F)GGGCTTTATCCTTTCCGTGT, PAI-2(R)GTGTGTCTTTGCTGATCCAC, 36B4(F)CAGGCCCTGCACTCTCGCTTTCTG, 36B4(R)TTGGTTGCTTTGGCGGGATTAGTC, p21(F)GTCAGGCTGGTCTGCCTCCG, p21(R)CGGTCCCGTGGACAGTGAGCAG. Primers used to detect Dicer transcripts include exon 9 and 10-F-GGTGGTTCGTTTTGATTTGCC, R-GGCAGTGTTGATTGTGACTC, Dicer exon14 and 16-F-CCGACCAGCCTTGTTACCTG, R-CGGTGTTTCCTTTGAATACTT, and Dicer exon18 and 19-F-GGGAAAGTCTGCAGAACAAAC, R-GGCTGTCTGAGCTCTTAGTTC.

Quantitative PCR of miRNA

Total RNA was isolated from empty pBABE and Cre pBABE retrovirus infected Dicer$^{c/c}$ MEFs by Trizol (Invitrogen). Reverse transcription of 1, 10, and 100 ng of total RNA with primers corresponding to each miRNA and the internal control U6b small nuclear RNA was performed as directed by the protocol of the two-step TaqMan MicroRNA Assay kit (Applied Biosystems). The second step included PCR amplification of duplicate cDNA samples with a fluorescent probe and fluorescent primers specific for each miRNA and U6b at the temperatures and times indicated in the protocol. All reactions were performed on an iCycler PCR instrument (Bio-Rad Laboratories). The expression of each miRNA from each sample was normalized to the expression of U6b, and the values of the Cre-expressing samples were compared with the values of the control infected samples, which were set at one. Error bars represent one standard deviation of the means of the normalized samples.

Image acquisition

Whole mount photographic images of embryos (Figs. 1 C and 4 A) were obtained using a stereoscope (MZ8; Leica) with either a 1X or 0.63X reduction lens and a 3008 Prog/Res digital camera coupled to a MacIntosh G4 computer, using Photoshop 4 software (Adobe). Images of tissue culture cells (Fig. 2 D and 3 G) were obtained using an inverted microscope (Carl Zeiss, Inc.) and a 3008 Prog/Res digital camera coupled to a MacIntosh G4 computer, using Photoshop 4 software (Adobe). Fig. 2 D was captured at 160X and 420X, whereas Fig. 3 G was captured at 420X. Histological images (Figs. 4 C and S3 B) were captured at 200X and 100X, respectively, using a microscope (BX41TF; Olympus) equipped with an Evolution MP5.0 camera (Media Cybernetics, Inc.), a Dell computer, and QCapture Pro (5.1.1.14) software into Photoshop 7 software. DAPI-stained cells (Fig. 2 F) were imaged using a microscope (Axioplan; Carl Zeiss, Inc.) with a 100X Neofluor 1.4 N.A. objective and a CCD digital camera captured with Axiovision software.

Staining for SA-βGal in developing embryos and in tissue

Analysis of *SA-βGal* activity was performed as described previously (www.med.upenn.edu/mcrc/epstein_lab/documents/Beta-GalactosidaseStainingOfEmbryos.doc).

Online supplemental material

Fig. S1 shows that Dicer loss induces early embryonic lethality, and that Cre-mediated excision of a conditional Dicer allele in MEFs results in loss of mature miRNA molecules. Fig. S2 demonstrates that Cre induction does not induce cell death or senescence in cells that retain Dicer or in Dicer-ablated cells lacking Ink4A/Arf. Fig. S3 shows that CAG-CreER or K5-Cre mediates Dicer excision in vivo. Online supplemental material is available at http://www.jcb.org/cgi/content/full/jcb.200802105/DC1.

We thank Dennis Roop and Robert Finberg for providing K5-CrePR mice and CAG-CreER mice, and Carlo Croce for assistance with miRNA arrays. 129S-*Gt(ROSA)26Sor*^{tm1Sor}/J mice were obtained from Jackson Laboratories. We thank Marilyn Keeler and Kathy Hoover for technical assistance, Hong Zhang for discussions, Roger Davis for Ras antibody, and Charlene Baron for help with figures.

This work was supported by grants from the American Heart Association to R. Mudhasani (0625823T), and the National Institutes of Health to C.M. Eischen (CA098193) and to S.N. Jones (DK73324, CA77735).

The authors have no conflicts of interest to declare.

Submitted: 18 February 2008
Accepted: 30 May 2008

References

Andl, T., E.P. Murchison, F. Liu, Y. Zhang, M. Yunta-Gonzalez, J.W. Tobias, C.D. Andl, J.T. Seykora, G.J. Hannon, and S.E. Millar. 2006. The miRNA-processing enzyme dicer is essential for the morphogenesis and maintenance of hair follicles. *Curr. Biol.* 16:1041–1049.

Bernstein, E., S.Y. Kim, M.A. Carmell, E.P. Murchison, H. Alcorn, M.Z. Li, A.A. Mills, S.J. Elledge, K.V. Anderson, and G.J. Hannon. 2003. Dicer is essential for mouse development. *Nat. Genet.* 35:215–217.

Bommer, G.T., I. Garin, Y. Feng, A.J. Kaczorowski, R. Kuick, R.E. Love, Y. Zhai, T.J. Giordano, Z.S. Qin, B.B. Moore, et al. 2007. P53-mediated activation of miRNA34 candidate tumor suppressor genes. *Curr. Biol.* 17:1298–1307.

Braig, M., S. Lee, C. Loddenkemper, C. Rudolph, A.H. Peters, B. Schlegelberger, H. Stein, B. Dorken, T. Jenuwein, and C.A. Schmitt. 2005. Oncogene-induced senescence as an initial barrier in lymphoma development. *Nature.* 436:660–665.

Brueckner, B., C. Stresemann, R. Kuner, C. Mund, T. Musch, M. Meister, H. Sultmann, and F. Lyko. 2007. The human let-7a-3 locus contains an epigenetically regulated microRNA gene with oncogenic function. *Cancer Res.* 67:1419–1423.

Campisi, J. 2003. Analysis of tumor suppressor gene-induced senescence. *Methods Mol. Biol.* 223:155–172.

Chang, T.C., D. Yu, Y.S. Lee, E.A. Wentzel, D.E. Arking, K.M. West, C.V. Dang, A. Thomas-Tikhonenko, and J.T. Mendell. 2008. Widespread microRNA repression by Myc contributes to tumorigenesis. *Nat. Genet.* 40:43–50.

Chen, Z., L.C. Trotman, D. Shaffer, H.K. Lin, Z.A. Dotan, M. Niki, J.A. Koutcher, H.I. Scher, T. Ludwig, W. Gerald, et al. 2005. Crucial role of p53-dependent cellular senescence in suppression of Pten-deficient tumorigenesis. *Nature.* 436:725–730.

Dimri, G.P., X. Lee, G. Basile, M. Acosta, G. Scott, C. Roskelley, E.E. Medrano, M. Linskens, I. Rubeli, O. Pereira-Smith, et al. 1995. A biomarker that identifies senescent human cells in culture and in aging skin in vivo. *Proc. Natl. Acad. Sci. USA.* 92:9363–9367.

Donehower, L.A., M. Harvey, B.L. Slagle, M.J. McArthur, C.A. Montgomery, J.S. Butel, and A. Bradley. 1992. Mice deficient for p53 are developmentally normal but susceptible to spontaneous tumours. *Nature.* 356:215–221.

Du, T., and P.D. Zamore. 2005. microPrimer: the biogenesis and function of microRNA. *Development.* 132:4645–4652.

Harfe, B.D., M.T. McManus, J.H. Mansfield, E. Hornstein, and C.J. Tabin. 2005. The RNaseIII enzyme Dicer is required for morphogenesis but not patterning of the vertebrate limb. *Proc. Natl. Acad. Sci. USA.* 102:10898–10903.

Harris, K.S., Z. Zhang, M.T. McManus, B.D. Harfe, and X. Sun. 2006. Dicer function is essential for lung epithelium morphogenesis. *Proc. Natl. Acad. Sci. USA.* 103:2208–2213.

Hayashi, S., and A.P. McMahon. 2002. Efficient recombination in diverse tissues by a tamoxifen-inducible form of cre: a tool for temporally regulated gene activation /inactivation in the mouse. *Dev. Biol.* 244:305–318.

He, L., X. He, L.P. Lim, E. de Stanchina, Z. Xuan, Y. Liang, W. Xue, L. Zender, J. Magnus, D. Ridzon, et al. 2007. A microRNA component of the p53 tumour suppressor network. *Nature.* 447:1130–1134.

Jackson, J.G., and O.M. Pereira-Smith. 2006. p53 is preferentially recruited to the promoters of growth arrest genes p21 and GADD45 during replicative senescence of normal human fibroblasts. *Cancer Res.* 66:8356–8360.

Johnson, S.M., H. Grosshans, J. Shingara, M. Byrom, R. Jarvis, A. Cheng, E. Labourier, K.L. Reinert, D. Brown, and F.J. Slack. 2005. Ras is regulated by the let-7 microRNA family. *Cell.* 120:635–647.

Kanellopoulou, C., S.A. Muljo, A.L. Kung, S. Ganesan, R. Drapkin, T. Jenuwein, D.M. Livingston, and K. Rajewsky. 2005. Dicer-deficient mouse embryonic stem cells are defective in differentiation and centromeric silencing. *Genes Dev.* 19:489–501.

Kortlever, R.M., P.J. Higgins, and R. Bernards. 2006. Plasminogen activator inhibitor-1 is a critical downstream target of p53 in the induction of replicative senescence. *Nat. Cell Biol.* 8:877–884.

Kumar, M.S., J. Lu, K.L. Mercer, T.R. Golub, and T. Jacks. 2007. Impaired microRNA processing enhances cellular transformation and tumorigenesis. *Nat. Genet.* 39:673–677.

Muljo, S.A., K.M. Ansel, C. Kanellopoulou, D.M. Livingston, A. Rao, and K. Rajewsky. 2005. Aberrant T cell differentiation in the absence of Dicer. *J. Exp. Med.* 202:261–269.

Murchison, E.P., J.F. Partridge, O.H. Tam, S. Cheloufi, and G.J. Hannon. 2005. Characterization of Dicer-deficient murine embryonic stem cells. *Proc. Natl. Acad. Sci. USA.* 102:12135–12140.

Narita, M., S. Nunez, E. Heard, M. Narita, A.W. Lin, S.A. Hearn, D.L. Spector, G.J. Hannon, and S.W. Lowe. 2003. Rb-mediated heterochromatin formation and silencing of E2F target genes during cellular senescence. *Cell.* 113:703–716.

Raver-Shapira, N., E. Marciano, E. Meiri, V. Spector, N. Rosenfeld, N. Moskovits, Z. Bentwich, and M. Oren. 2007. Transcriptional activation of miR-34a contributes to p53-mediated apoptosis. *Mol. Cell.* 26:731–743.

Serrano, M., H. Lee, L. Chin, C. Cordon-Cardo, D. Beach, and R.A. DePinho. 1996. Role of the INK4a locus in tumor suppression and cell mortality. *Cell.* 85:27–37.

Sharpless, N.E., M.R. Ramsey, P. Balasubramanian, D.H. Castrillon, and R.A. DePinho. 2004. The differential impact of p16(INK4a) or p19(ARF) deficiency on cell growth and tumorigenesis. *Oncogene.* 23:379–385.

Volinia, S., G.A. Calin, C.G. Liu, S. Ambs, A. Cimmino, F. Petrocca, R. Visone, M. Iorio, C. Roldo, M. Ferracin, et al. 2006. A microRNA expression signature of human solid tumors defines cancer gene targets. *Proc. Natl. Acad. Sci. USA.* 103:2257–2261.

Voorhoeve, P.M., C. le Sage, M. Schrier, A.J. Gillis, H. Stoop, R. Nagel, Y.P. Liu, J. van Duijse, J. Drost, A. Griekspoor, et al. 2006. A genetic screen implicates miRNA-372 and miRNA-373 as oncogenes in testicular germ cell tumors. *Cell.* 124:1169–1181.

Webley, K., J.A. Bond, C.J. Jones, J.P. Blaydes, A. Craig, T. Hupp, and D. Wynford-Thomas. 2000. Posttranslational modifications of p53 in replicative senescence overlapping but distinct from those induced by DNA damage. *Mol. Cell. Biol.* 20:2803–2808.

Yang, W.J., D.D. Yang, S. Na, G.E. Sandusky, Q. Zhang, and G. Zhao. 2005. Dicer is required for embryonic angiogenesis during mouse development. *J. Biol. Chem.* 280:9330–9335.

Ye, X., B. Zerlanko, R. Zhang, N. Somaiah, M. Lipinski, P. Salomoni, and P.D. Adams. 2007. Definition of pRB- and p53-dependent and -independent steps in HIRA/ASF1a-mediated formation of senescence-associated heterochromatin foci. *Mol. Cell. Biol.* 27:2452–2465.

Zhang, H. 2007. Molecular signaling and genetic pathways of senescence: its role in tumorigenesis and aging. *J. Cell. Physiol.* 210:567–574.

Zhou, Z., D. Wang, X.J. Wang, and D.R. Roop. 2002. In utero activation of K5.CrePR1 induces gene deletion. *Genesis.* 32:191–192.